https://doi.org/10.1016/j.compositesb.2016.03.041

Rapid Microwave Sintering of Carbon Nanotube-Filled AZ61 Magnesium Alloy Composites

Akeem Damilola Akinwekomi, Wing-Cheung Law, Chak-Yin Tang*, Ling Chen, and Chi-Pong Tsui,
Department of Industrial and Systems Engineering, The Hong Kong Polytechnic University,
Hung Hom, Kowloon, Hong Kong, China
* Corresponding author. Tel.: +(852)2766 6608; Fax: +(852)2362 5267;
E-mail address: *cy.tang@polyu.edu.hk

Abstract

In this study, a powder metallurgy processing technique combined with rapid microwave sintering was used to synthesise carbon nanotubes (CNTs) filled AZ61 magnesium alloy composites under ambient conditions, without recourse to any secondary process. In order to determine the appropriate amount of CNTs for taking full advantage of the CNTs/AZ61 composite, a powder mixture of the CNTs, in varying volume fractions of 1 - 3%, and the AZ61 was prepared through a mechanical milling process. The optimized milling intensity allowed for reducing the powder size for effective microwave absorption, and thus improved the dispersion of the CNTs in the Mg alloy matrix without reducing the structural integrity of CNTs. In addition to the incorporation of the CNTs with the dual role of mechanical reinforcement and microwave susceptor, microwave sintering was achieved in only 8 minutes by using a synergetic combination of graphite and silicon carbide as microwave susceptors in a microwave furnace. The sintered samples, whose porosity ranged between 4 and 6 %, were characterised for microstructural, hardness, compressive and fracture properties. The results of hardness and compression tests indicated that these properties of all the composites were significantly improved compared to the monolithic samples. The highest microhardness value (~105 % increment) was recorded for the composite with 3.0% volume fraction of CNTs, while the composite sample with 1.0% volume fraction of CNTs had the highest ultimate compressive yield strength and 0.2% offset yield strength with approximate increments of 59 % and 127 %, respectively. The failure mechanisms of the composites as compared with the monolithic samples were discussed.

Keywords: A. Metal-matrix composites (MMCs) B. Mechanical properties E. Powder processing E. Sintering

1. Introduction

Lightweight structural materials with enhanced mechanical and physical properties are being continuously developed to cater for the increasingly stringent conditions required for weight and energy savings in many structural applications. Magnesium (Mg), as the lightest structural material, has attracted great attention from researchers not only as a result of its low density but also its high damping capacity and high strength-to-weight ratio. However, it suffers from poor ductility, limited strength and hardness when compared to other widely used structural materials such as aluminium (Al) and steel. Thus, considerable research efforts are being expended to increase its strength and ductility by alloying with other metals and reinforcing with fibres and particles [1–3].

Ever since being discovered, carbon nanotubes (CNTs) have received a lot of attention from researchers for serving as a reinforcing material in composites, because of numerous distinctive advantages such as low density, good electrical and thermal conductivities, extraordinary mechanical properties, and high aspect ratio. Several studies have been focused on CNT filled polymer composites [4-7]; however, relatively less work has been done on the processing and characterization of CNT filled metal composites, although CNTs could highly impede dislocation movement in the metal matrix [8-11]. Although the CNT filled composites have shown improved strength and toughness [7-8], achieving a good bonding between the matrix and CNTs [14], a homogeneous dispersion of the CNTs as well as protecting their structural integrity during processing are some of the main challenges yet to be overcome for further enhancing their properties [12-13]. Although fairly good dispersion has been realized using mechanical ball milling, the CNTs could also be damaged in the process due to a lack of

process optimisation and high milling intensity [12-13, 15] and thus the damaged CNTs could adversely affect the strength of the resulting composites.

The powder metallurgy (PM) technique is advantageous in processing Mg alloys and their composites, because of its suitability for a wide range of alloy types, and its ability for incorporating high volume fractions of the reinforcing phase in the matrix, minimisation of deleterious matrix-reinforcement reactions and the production of net or near-net shaped parts [16]. Moreover, PM could even become more advantageous if the subsequent consolidation step in the sintering could be done faster and cleaner, with minimal porosity and defects in the final product [12-13]. In view of this, the microwave (MW) sintering technique has been promoted as a candidate for a consolidation method that can fulfil these conditions.

MW is an eco-friendly technology which can realise rapid heating rates, enhance diffusion processes and microstructural uniformity, as well as reduce energy consumption, save time and cost without compromising material properties [17-18]. It has been used in a wide range of industrial processes including drying, calcinations, chemical synthesis, food processing and material sintering [18]. Several years before, for microwave sintering, most of the research mainly focused on ceramics because metals could not be significantly heated by microwave as they reflect most of the microwaves and have limited penetration depths of a few microns [19]. However, it has been reported that powdered metals can be heated efficiently and effectively using microwave energy [20]. Later, microwave has been applied in many metallurgical applications, such as sintering of various metals and composites [21-22]. Recently, certain attempts have been made to fabricate magnesium based composites reinforced with CNTs [23] or hybrid CNTs based nano-particles, such as CNT-silicon carbide (CNT-SiC) [24], CNT-aluminium (CNT-Al) [25] and CNT-alumina (CNT-Al_2O_3) [26] through MW sintering. However, the processing of CNT filled magnesium alloy (e.g. AZ61) based composites through MW sintering has not yet been reported. On the other hand, there have been few studies on the enhancement of mechanical properties of Mg/(CNT-Al) and Mg/(CNT-

SiC) composites by using the PM technique with MW sintering as a primary processing followed by an extrusion process [24-26]. As extrusion can significantly enhance the mechanical properties of metal matrix composites through matrix grain refinement and the generation of a strong texture [27], one might argue that the mechanical improvement was mainly attributed to the extrusion process instead of the reinforcement conferred by the CNTs. Moreover, no report on the microstructure, hardness, and compressive properties of the CNT filled magnesium alloy composites fabricated by MW sintering without post processing has been found in the open literature.

It has also been known that CNTs are good microwave susceptors [28-29] for the MW sintering process, and good reinforcing fillers for enhancing the mechanical properties of the resulting composites [23-26]. In addition, SiC can serve as a susceptor material in Mg/(CNT-SiC) composites during MW sintering [24], leading to reduction of the processing time. However, the blend-press-sinter technique utilised in their works resulted in clustering of the reinforcement, limiting the weight fraction of CNTs that could be incorporated in the matrix to 1 wt.% [25]. Moreover, the blending/mixing technique is not an efficient method for dispersing nanoparticles due to the persistence of CNTs clusters in the matrix [13]. This fact was also corroborated in the work [26], in which MW sintered composites processed by mixing CNTs with the Mg matrix were characterised by poor surface finish, easy edge-chipping, and reduction in failure strain, due to cluster formation of the CNTs and poor bonding between the CNTs and Mg [26].

In this study, the PM processing technique combined with rapid MW sintering was used to fabricate AZ61/CNT composites without recourse to any secondary/post-processing plastic deformation process such as extrusion. The synergetic effects of a mixture of silicon carbide (SiC) and graphite as MW susceptors, coupled with the dual functions of the CNTs, were investigated. The effects of varying the proportion of CNTs on the microstructure, hardness,

compressive properties and compressive failure mechanisms of the microwave sintered AZ61/CNT composites are discussed.

2. Experimental procedures

2.1 Materials

The composition and characteristics of water atomized AZ61 magnesium alloy powder (150-300 μm, Tangshan Weihao Magnesium Powder Co., Ltd, China), whose composition and characteristics are shown in Table 1, was used as the raw material for the matrix of the composite. Multiwall carbon nanotubes synthesised by chemical vapour deposition (herein referred to as CNTs: purity >95 wt.%; internal diameter: 3-5 nm; outer diameter: 8-15 nm; length: ~50 μm), supplied by the Chinese Academy of Sciences, Chengdu Organic Chemistry Co., Ltd., China, were used as both the reinforcement phase and microwave susceptor [28,29].

2.2 Synthesis of AZ61/CNT composites and Raman Spectroscopy

The powder metallurgy technique was used for synthesising the monolithic and CNT-filled AZ61 magnesium alloy composites. CNTs were weighed and added to AZ61 powder so that four different classes of specimen were produced to yield CNT reinforcement volume fractions (vol.%) varying from 0 to 3 vol.% (designated as AZ61-*x*CNT where *x* is 1.0, 2.0, and 3.0 vol.%). The mixture of AZ61/CNT was milled at 300 rpm for 15 hours using a QM-3SP2 planetary ball mill, manufactured by the Nanjing University Instrument Plant, to reduce the powder size and to homogenise the mixture for effective microwave absorption. Two different sizes of ball (Ø 8 mm and Ø 15 mm), in equal weight proportion, were used for milling at a charge ratio of 20:1. A combination of different ball sizes in addition to a process control agent, has been reported to be effective in minimising cold welding and increasing the powder yield during milling [30]. In addition, the smaller balls can randomise the motion of the bigger ones [30] and reduce the impact force transferred to the AZ61/CNT mixture, which can be instrumental in preserving the structural integrity of the CNTs. 30 vol.% of cyclohexane was

also added to the powder mixture as a process control agent. In order to minimise the powder oxidation, the milling jar containing the powder mixture was evacuated for 20 minutes using a vacuum pump prior to the start of milling. The homogeneously mixed powder was thereafter put in a rigid die and compacted using a uniaxial compressive pressure of 500 MPa for a total of 300 seconds to form green cylindrical compacts with diameter and height of 15 mm and 14 mm, respectively.

Raman spectroscopy studies were also carried out on the as-received CNTs and the AZ61-2.0CNT composite to assess the integrity of the CNTs after the ball-milling operation. A Horiba Jobin Yvon (HR800) microspectrometer was used to measure the spectra of the samples under ambient conditions using a visible red excitation laser source of 632.8 nm. The incident power was 50 mW.

2.3 Microwave sintering process

The compacts were placed in a SiC/graphite lined crucible, as shown in Fig. 1, and sintered at 500 ^{o}C, close to the solidus temperature of the alloy, in a multimode microwave oven (6 kW, 2.45 GHz, Kailing Industrial Microwave Equipment Ltd., China). The sintering time was 8 minutes at a power of 1000 W. This sintering set-up allows a microwave assisted bi-directional sintering technique, the details of which have been reported in the literature [24-25]. In this work, a mixture of SiC and graphite was used for susceptors. Graphite has a higher loss tangent (average $\tan \delta = 0.59$ [28]) than SiC ($\tan \delta = 0.37$ [21]), implying that the latter has a higher efficiency in transforming absorbed microwaves into heat for further increasing the temperature of the compact until it couples directly with the microwaves. At temperatures above 250 °C, thermal oxidation of graphite begins to take place [31], reducing its conversion efficiency. On the other hand, SiC has a higher thermal resistance, which can counteract the reduced MW absorption and conversion ability of graphite. CNTs, due to the high loss tangent ($\tan \delta = 0.70$ [28]) are expected to not only act as reinforcement, but to also contribute to speed

up the sintering process [28-29]. The synergy between the three susceptors is expected to remarkably shorten the sintering time. Furthermore, in order to reduce the oxidation of the compacts during sintering, they were covered with AZ61 powder, which acted as a getter material [32].

2.4 Density and porosity measurement

The green density and sintered density of the compacts were calculated by dimensional measurements and Archimedes' principle, respectively. The theoretical densities of the composites were determined by the rule-of-mixture principle. The average value of three samples from each set was determined and reported. A measure of the densification that occurred during sintering was calculated by using a dimensionless parameter, the densification parameter (DP), as expressed in Eq. (1) [33]. A positive DP indicates shrinkage while a negative DP indicates swelling:

$$\text{Densification parameter} = \frac{\text{sintered density} - \text{green density}}{\text{theoretical density} - \text{green density}} \quad (1)$$

2.5 Microstructural examination and X-ray diffraction analysis

Microstructural examination was done on metallographically polished samples in order to study the morphology of the grains and pore structure using an optical microscope (Leica DM4000). The samples were polished using 240, 320, 400, 600, and 800 grit SiC grinding paper. Final mirror-like polishing was done using 2 μm-size oil-soluble polycrystalline diamond paste followed by 0.25 μm-size oil-soluble polycrystalline diamond paste. The etchant used was acetic picral (6g picric acid, 5ml acetic acid, 10ml water and 100ml ethanol). The phases present in the milled powder, sintered composites and monolithic samples were identified from X-ray diffractograms (Rigaku SmartLab 9KW XRD) by exposing them to Cu Kα radiation (λ = 1.54056Å) at a scanning speed of 4 deg/min.

2.6 Hardness test

The Vickers microhardness values of both monolithic and composite samples were determined according to ASTM E384-11[34] using a Mitutoyo HM-211 machine equipped with a diamond indenter. The applied load was 0.5 N for a 15-second dwell time. The mean of seven different readings was determined for each type of sample. The readings were taken at intervals of 1.5 mm across the surface of each of the samples.

2.7 Compression test

Compression tests were conducted at ambient temperature according to ASTM E9-09 [35] using a Material Test System machine (MTS 810) at a cross-head speed of 0.04 mm/min on samples with an aspect ratio (length : diameter) of 0.8. The 0.2% compressive yield strength (CYS), ultimate compressive strength (UCS), and failure strain of the samples were evaluated.

2.8 Fractography

Fracture surfaces from samples subjected to the compression tests were used for fractography characterisation to determine the mode and mechanisms of fracture using a scanning electron microscope (SEM), JEOL JSM-6490) and a field emission scanning electron microscope (FESEM, JEOL JSM-6335F).

3. Results and discussion

3.1 Composite synthesis and Raman spectroscopy

The powder metallurgy technique and 8-minute rapid hybrid-microwave sintering were used to successfully consolidate AZ61 magnesium alloy and its composites filled with multi-wall CNTs. From Fig. 2 (a), the average particle size of the as-received AZ61 magnesium alloy powders was 200 μm, which was successfully reduced to less than 100 μm by mechanical ball milling, as shown in Fig. 2 (b). It is important to homogeneously mix the AZ61 powder with CNTs and ensure the formation of good green compacts devoid of delamination cracks.

Furthermore, powdered metal compacts with particles less than 100 μm can effectively absorb microwaves at 2.45 GHz [36]. As shown in the high magnification SEM images in Fig. 2(c) and 2(d), no CNTs could be found on the surface of the AZ61 powder after milling for 15 hours, indicating that the CNTs had become embedded within the powder particles.

Esawi and co-workers [15] reported that CNTs became embedded within aluminium powder after milling the composite mixture for 6 hours. However, in this study, the use of steel balls with two different diameters as the milling media and a process control agent were effective in preventing the formation of the very large particles (> 1 mm) reported in [15] due to excessive cold welding of the aluminium powder. The large particles formed would have prevented effective consolidation in the subsequent processing steps. The smaller balls are expected to randomise the motion of the bigger ones [30], consequently the impact forces experienced by AZ61/CNT mixture, are reduced. In addition, the use of a relatively high charge ratio of 20:1 can also contribute to the reduction of the milling intensity and hence preserve the structural integrity of the CNTs due to the restricted movement of the balls in the milling vial [37].

In order to assess the structural integrity of the CNTs in the composite mixture after the mechanical ball milling process, the Raman spectra were obtained for different milling periods. From Fig. 3, two peaks appeared at 1352 and 1577 cm^{-1}, which correspond to the D-line (defect) and graphitic G-line, respectively, of the as-received CNTs. A measure of the structural integrity or damage to CNTs can be obtained by comparing the relative intensity between the two peaks i.e. the I_D/I_G ratio [13]. An increase in the ratio implies an increase in defect density (amorphization), indicating the occurrence of some damage. On the other hand, a decrease in the I_D/I_G ratio is an indication of graphitisation due to annealing. From the results in Table 2, the I_D/I_G ratio of the composites milled for 5 to 15 hours do not vary significantly as compared with that of the as-received CNTs. This indicated that damage of CNTs was not apparent during the mechanical milling operation. In addition to the use of milling media with different

diameters and a high charge ratio, the AZ61 powder particles may also act as impact absorbers [38] as soon as the CNTs became embedded within the particles (at 10 hours of milling) during the milling process. Although Choi et al. [38] reported that the CNTs in Al/CNT composites were slightly damaged after 6 hours while using milling balls of the same diameter, the processing method used in this study led to preserving the structural integrity of the CNTs.

3.2 Sintering and densification response

Unlike conventional sintering which requires a prolonged sintering time in excess of 3 hours and an inert atmosphere, only 8 minutes were required to achieve sintering in air in a microwave furnace. CNTs, apart from their reinforcement effect, are also expected to function as susceptor material [28-29] to convert microwave energy into heat energy and transfer it to the matrix during sintering. The synergetic effect of the SiC/graphite lined crucible and the CNTs resulted in rapid sintering due to the high heating rate; therefore, there was no need for the intermittent holding temperature required in conventional sintering. Although similar rapid sintering behaviour has been reported for some Mg-based systems [24-25], the sintering time in our work was considerably reduced by ~68% and ~38% compared to those reported in references [24] and [25], respectively. This can translate into substantial energy and time savings, as shown in Table 3.

The results of density, porosity, and the densification parameter calculations are presented in Table 4. The sintered densities of the composites and unfilled AZ61 alloy increased to more than 93% of the theoretical densities, indicating pore closure and densification. This is also confirmed by the positive values of the DP indicating sintering shrinkage as a result of pore closure. Porosity does not follow a definite trend, although the AZ61-3.0CNT sample had the highest porosity. CNTs have a higher density (2.6 g/cm^3) when compared to the density of the AZ61 matrix (1.80 g/cm^3); therefore, the experimental density of the samples increased as the amount of CNTs introduced into the matrix was increased.

3.3 Microstructural examination and X-ray diffraction analysis

Fig. 4 shows the optical microstructures of the microwave sintered AZ61 alloy and its composites. The average grain size of the unfilled matrix in Fig. 4(a) was 11.7 ± 2.4 μm. However, as CNTs were added to the matrix, the composites exhibited significant larger grain sizes, as shown in Fig. 4(b) - 4(d). The largest average grain size of 35.0 ± 14.0 μm was observed in the AZ61-3.0CNT sample (Fig. 4(d)). Furthermore, as shown in the micrographs, there is no obvious grain refinement due to the presence of CNTs in the matrix, which is similar to the results reported by Goh and co-workers for a Mg/CNT composite [39].

Although, matrix grain-refinement was reported in [25,39-40], it could not be solely credited to the nano-reinforcement because the composites were subjected to extrusion. Extrusion is an example of a secondary processing plastic deformation technique which is used to enhance the mechanical properties of alloys and composites through matrix grain refinement and the generation of dislocations [41]. From Table 5, the grain sizes in the composite samples are bigger and show a larger size distribution compared to the unfilled matrix. A plausible explanation of this observation can be attributed to the CNTs which were added to the matrix. CNTs may function as nucleation loci within the matrix [16] and also have the capability of absorbing and converting microwave energy to heat energy [28], which can lead to localised heating and subsequent localised grain growth.

The XRD profiles of the as-received AZ61 powder, milled AZ61/CNT powder mixture and sintered composites are presented in Figs. 5(a) and 5(b), respectively. No carbon peak was detected in any of the samples and could have resulted from the limitation of the X-rays in identifying elements with very low concentrations [42]. In addition to the peaks for the Mg matrix, which were identified in all the samples, the peaks of an intermetallic compound $Al_{12}Mg_{17}$ were present at $2\theta = 35.95°$, 39.88°, and 43.53° in the as-received and milled powder. We opine that the compound may have been carried over from the powder production process.

However, in the sintered samples, many of the peaks identified as $Al_{12}Mg_{17}$ in the powder samples disappeared, indicating that they must have gone into solid-solution during the sintering process. Furthermore, the peaks of another intermetallic compound, identified as $Al_{77}Mn_{23}$, are also seen at $2\theta = 43.02°$ and 62.09° in all the sintered samples. An unidentified peak at $2\theta = 54.5°$, which is clearly absent in the sintered monolithic alloy, is observed in all the sintered composite samples. In a PM processed Mg/CNT composite [43], a similar unidentified peak at $2\theta = 54.35°$ is observed. The authors rationalised and assigned it to a ternary magnesium carbide with the chemical formula of Al_2MgC_2. The formation of a ternary Mg-carbide (Al_2MgC_2) in a carbon fibre reinforced Mg-alloy containing 0.6 - 19 wt.% of aluminium at a temperature greater than 700 ^oC with a prolonged heating of more than 20 hours has been reported [44]. Considering the short microwave sintering time in this work, we are hesitant to assign the unidentified peak to the ternary Mg-carbide. Further investigations are needed to definitively identify it.

3.4 Hardness test

The microhardness values of both the monolithic and composite samples are shown in Table 5. The results show that the microhardness value increased significantly as a result of the incorporation of CNTs into the AZ61 matrix. Generally, the microhardness value increased with increasing CNT volume fraction in the matrix, peaking at 3.0 vol.% (>100%). This increase in hardness can be attributed to a fairly uniform dispersion of the CNTs in the matrix and an increased resistance to localised deformation of the matrix during indentation as a result of the reinforcement phase [25]. Some researchers have reported similar observations in spray formed and extruded AZ61/nano silica (n-SiO_2) composites [40] and Mg/CNT composites [25]. Although extrusion was not undertaken on the samples in the present study, the microhardness value of AZ61-3.0CNT (86.9 HV) compared favourably with the 88 HV reported for cast and extruded AZ61/n-SiO_2 in reference [40]. This also indicates the suitability

of microwave sintering and the processing parameters used in this study for consolidating PM processed Mg-based composites.

3.5 Compression test

The compression test results in Table 5 indicate that the CNTs in the AZ61 matrix resulted in improved ultimate compression strength (UCS) and 0.2% compression yield strength (0.2% CYS). The values of UCS of the composites were significantly higher than those of the monolithic matrix sample. Monolithic AZ61 had a UCS of 135.5 MPa while AZ61-2.0CNT, which had the lowest UCS of 210.7 MPa among the composite samples, exhibited a significant increment of ~55% compared to the monolithic alloy. The highest UCS exhibited by the AZ61-1.0CNT (307.1 MPa) was more than double the value recorded for the monolithic alloy (135.5 MPa). A similar trend was also observed for the 0.2% CYS. Some researchers [3,40,45] have reported similar improvements in the mechanical properties of Mg-based and Al-based composites, which were rationalised based on a number of strengthening factors, including the Orowan strengthening mechanism arisen from the obstruction of dislocation movement by the CNTs [16,40,46], the matrix-reinforcement thermal and elastic moduli mismatch which increases dislocation density and hence, increases strength [16,45-46] (CTE of Mg = 28.5 X 10^{-6} K^{-1} [21]; CTE of CNTs = 2.7 X 10^{-6} K^{-1} [44]), strong bonding between the matrix and CNTs [48-49], and efficient load transfer from the matrix to the reinforcement [3,16,46]. All the composite samples showed higher failure strains compared to the unfilled matrix, except for the sample AZ61-3.0CNT which had a similar level of failure strain as the monolithic AZ61 alloy. The highest strain was 12.5% for AZ61-2.0CNT which was ~23% greater. The presence of CNTs in the matrix can activate non-basal slip systems in the matrix [25], thereby improving the failure strains of the composites. This further suggests that the clustering of CNTs was minimised by using the adopted processing parameters. Reinforcement clustering has been reported to compromise the mechanical properties of the composites [3].

Although the sintering time utilised in the present work was significantly shortened, this has not compromised the compressive properties of the samples.

3.6 Fractography

SEM and FESEM images of the fractured surfaces of the unfilled AZ61 and its composites with 3 vol.% of CNTs are presented in Fig.6. Macroscopic examination of the failed samples after compression tests showed that failure occurred along cracks angled at ~45^{o} to the compression axis (insets in Fig.6(a) and Fig.6(b)). The monolithic sample fractured along two cracks (inset in Fig.6(a)) while the composite samples failed along a single principal crack (inset in Fig.6(b)). From Fig.6(a), the monolithic alloy shows a relatively smooth fracture surface due to twinning shear. Moreover, few microvoids with one labelled "X" in Fig.6(a)) were present along the shear bands, implying that one of the failure mechanisms for the unfilled AZ61 may be linked to void formation and growth [49]. For the composite sample with 1 vol.% of CNTs as shown in Fig.6(b), it shows relatively rough and jagged surfaces, suggesting a mixed mode of shear and brittle failure. These observations are consistent with the results of Habibi et al. [25] for a Mg/CNTs composite. Furthermore, high resolution FESEM image of the fracture surfaces of the composite showed a microcrack (labelled "Y" in Fig.6(c)) formed around localised CNTs due to the stress concentration, implying that the CNTs may act as sites for crack initiation and subsequent crack propagation in the surrounding AZ61. Therefore, the failure mechanism of the composites was highly influenced by the matrix/CNTs interface, matrix cracking, and CNTs fracture.

4. Conclusions

Carbon nanotube-filled AZ61 magnesium alloy composites were successfully synthesised using the powder metallurgy processing technique combined with rapid microwave sintering. Mechanical ball milling with an optimized milling intensity was found to be effective in incorporating the CNTs into the AZ61 matrix without undermining the structural integrity

of CNTs as reflected from the Raman Spectroscopy results. With the CNTs incorporated into the AZ61 matrix, as well as a combination of graphite and SiC susceptors in a microwave furnace, the proposed sintering process was completed rapidly in 8 minutes. As compared with the monolithic samples, the microwave sintered composite samples showed significant improvement not only in the hardness (~105 % increment for the samples with 3 vol.% CNT), but also in the compressive properties (~59% increment and ~129% for the compressive strength and 0.2% offset compressive yield strength of the samples with 1 vol.% of CNT, respectively) of the composites, without compromising their failure strain. The failure mechanism in the monolithic alloy was mainly involved void formation and growth, while the composites exhibited a mixed mode of shear and brittle fracture. Lightweight Mg-based nanocomposites have a number of potential applications in the military and aviation fields. Our work contributes to a rapid sintering method that can prepare Mg-based components by a powder metallurgy route.

Acknowledgements

The work described in this study was supported by the Hong Kong PhD Fellowship Scheme (HKPFS) of the Research Grants Council, RGC, The Government of the Hong Kong Special Administrative Region (Project Code: 1-904Z).

Table 1 Chemical composition and physical properties of AZ61 magnesium alloy powder

Composition (wt.%)	Mg:86.36, Al:5.86, Zn:0.69, Mn:0.29,O:6.80,
Processing route	Water atomization
Particle size (μm)	
D_{10}	129.10
D_{50}	173.51
D_{90}	240.16
Specific surface area (m^2/g)	0.013
Theoretical density (g/cm^3)	1.80

Table 2 Raman spectra characteristics of as-received CNTs and AZ61-2.0CNTs mixture for different milling durations.

Milling time (h)	0	5	10	15
I_D/I_G **ratio**	0.8572	0.8557	0.8592	0.8590

Table 3 Comparison of energy and time savings between the present work and other reports of Mg-based microwave sintering.

Matrix	**MW Sintering power (kW)**	**Time (minutes)**	**Energy consumed kWh**	**Energy* saved (%)**	**Time* saved (%)**	**Reference**
Mg	0.9	25	0.38	-	-	[24]
Mg	0.9	13	0.20	70	48	[25]
AZ61	1.0	8	0.13	81	68	Present work

- *calculated as compared with ref.[24]*

Table 4 Results of density, porosity, and densification parameter measurements

Sample	**CNTs (vol.%)**	**Theoretical density (g/cm^3)**	**Green density (g/cm^3)**	**Sintered density (g/cm^3)**	**Porosity**	**Densification parameter (DP)**
AZ61	0	1.800	1.573 ± 0.011	1.691 ± 0.015	6.03	0.520
AZ61-1.0CNT	1	1.803	1.588 ± 0.003	1.733 ± 0.041	3.90	0.778
AZ61-2.0CNT	2	1.806	1.595 ± 0.005	1.692 ± 0.064	6.32	0.455
AZ61-3.0CNT	3	1.809	1.594 ± 0.007	1.699 ± 0.005	6.06	0.491

Table 5 Results of grain size, microhardness and compressive properties at room temperature

Sample	**CNTs (vol.%)**	**Grain size (μm)**	**Microhardness (HV)**	**0.2% CYS (MPa)**	**UCS (MPa)**	**Failure strain (%)**
AZ61	0	11.7 ± 2.4	42.4 ± 3.7	110.4 ± 8.9	135.5 ± 3.3	10.2 ± 1.5
AZ61-1.0CNT	1	21.4 ± 8.7	61.8 ± 8.6	175.8 ± 29.6	307.1 ± 13.4	11.4 ± 2.3
AZ61-2.0CNT	2	24.0 ± 8.8	71.1 ± 7.2	133.7 ± 13.5	210.7 ± 16.2	12.5 ± 0.2
AZ61-3.0CNT	3	35.0 ± 14.0	86.9 ± 10.3	116.9 ± 6.7	217.9 ± 23.5	10.2 ± 0.8

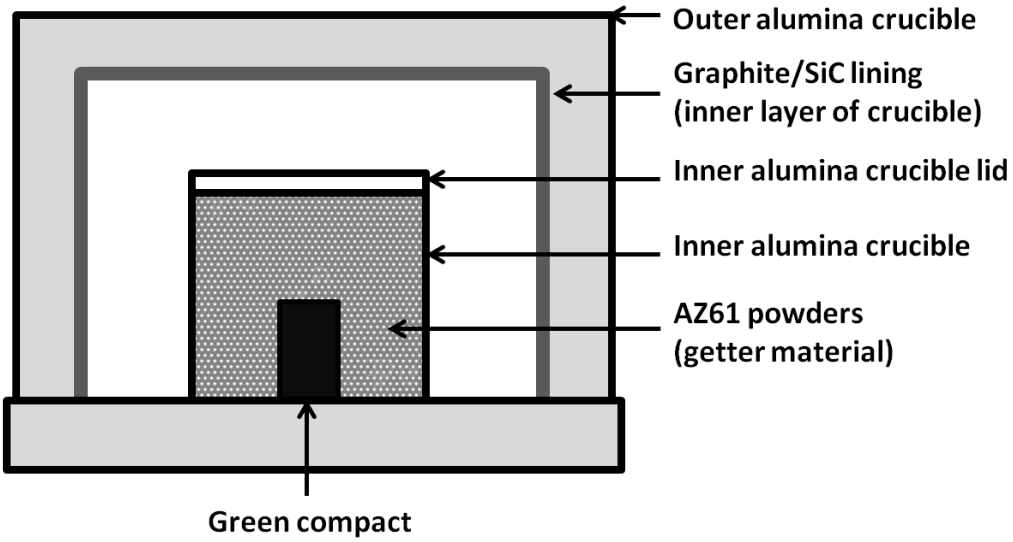

Fig.1 Cross-sectional view of the silicon carbide/graphite lined crucible and the position of a compact during microwave sintering.

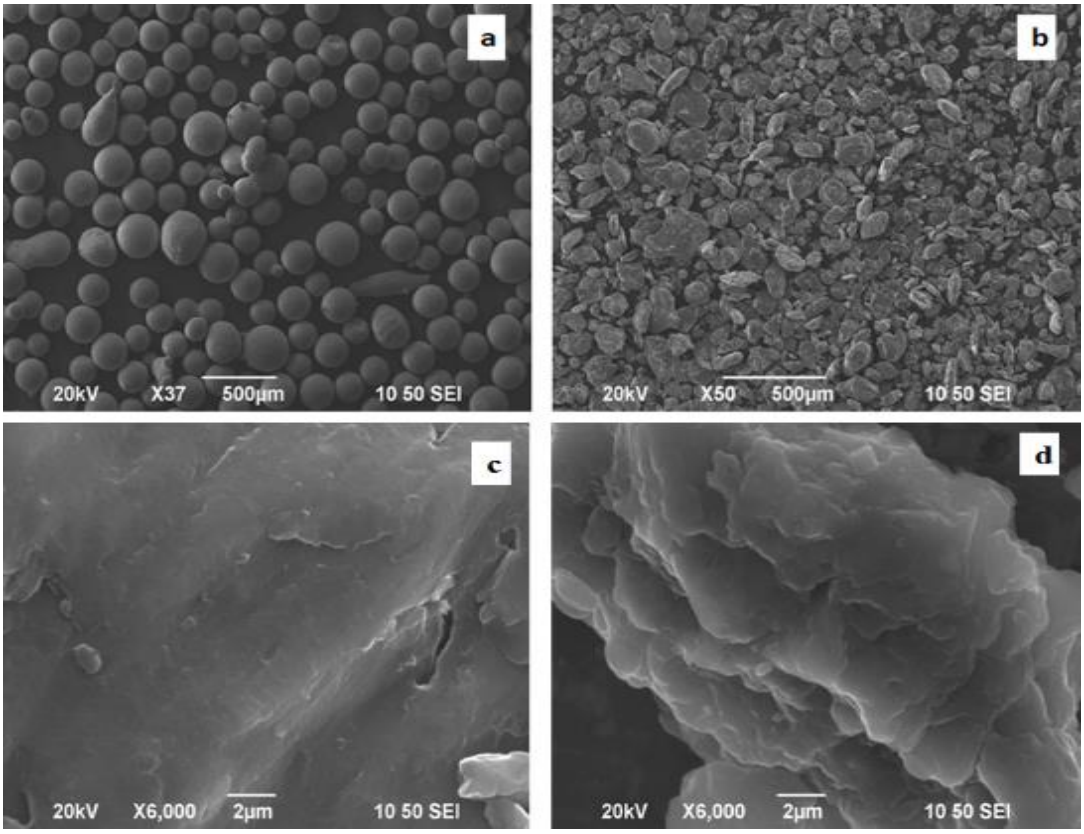

Fig. 2 SEM micrographs of AZ61 alloy (a) as-received mainly spherical powder particles, (b) after 15 hours of milling showing flattened flake-like particles; and high magnification SEM images of (c) surface of AZ61-2.0CNT after 15 hours of milling, and (d) surface of AZ61-3.0CNT after 15 hours of milling.

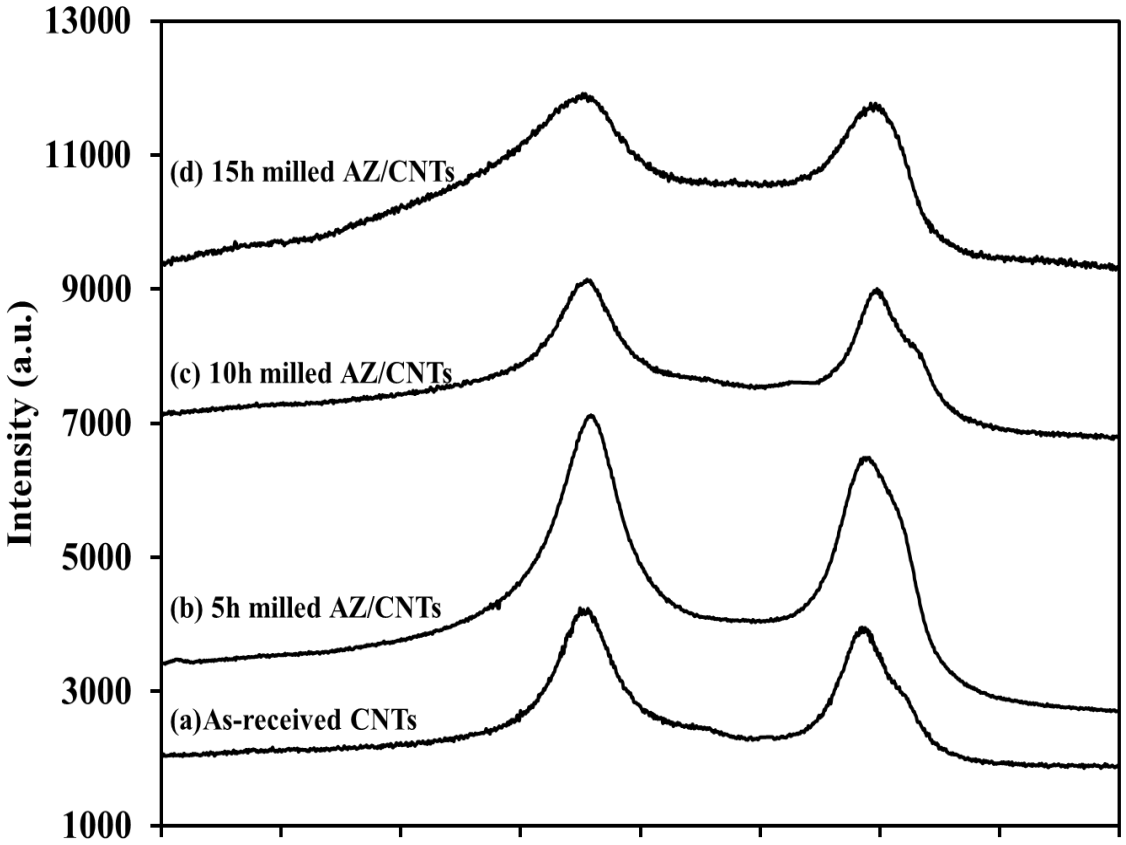

Fig.3 Raman spectra of (a) as-received CNTs; and AZ61-2.0CNTs milled for (b) 5 hours; (c) 10 hours; and (d) 15 hours

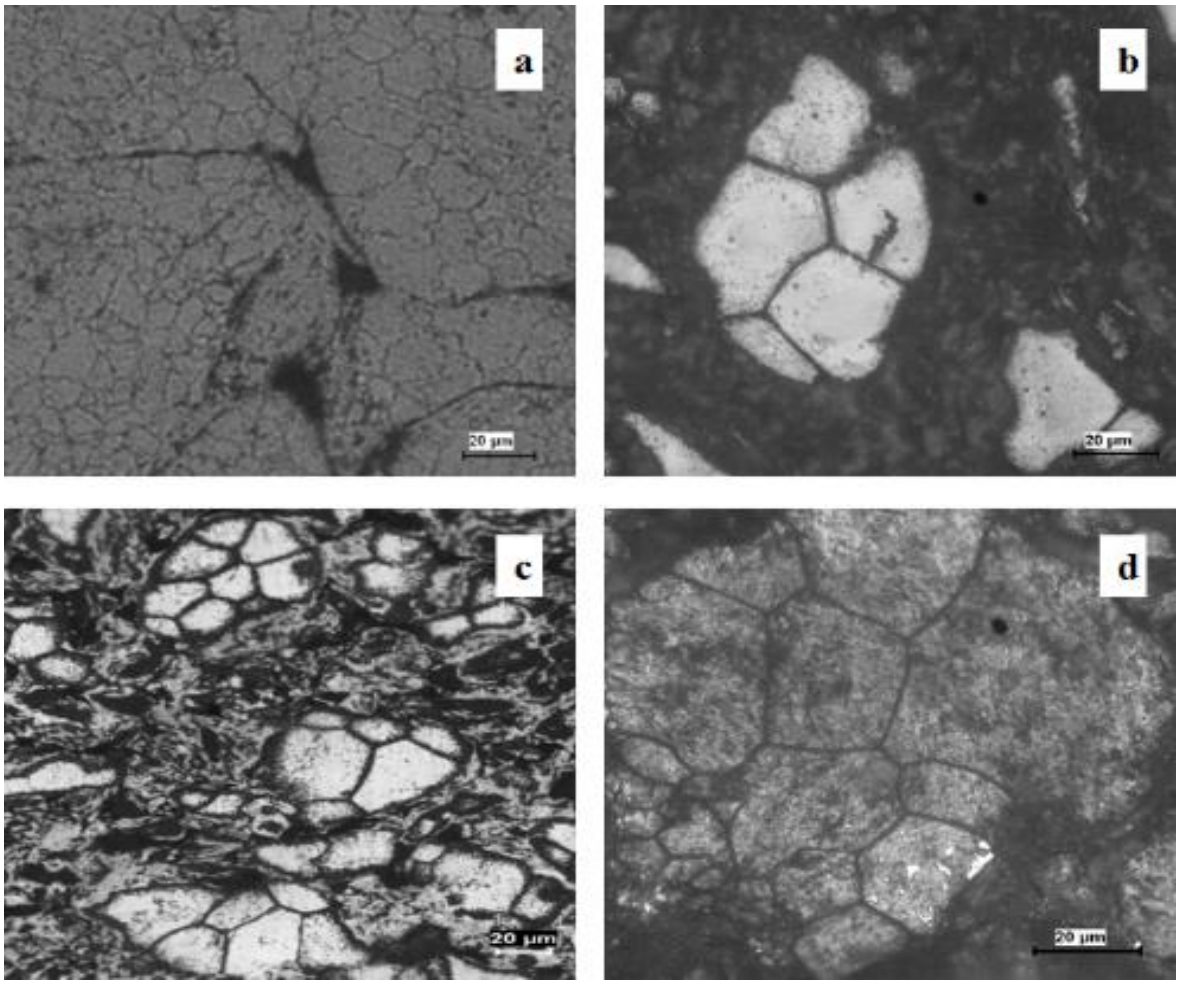

Fig.4 Optical microstructures of the grain structure for a (a) monolithic AZ61; (b) AZ61-1.0CNT; (c) AZ61-2.0CNT; and (d) AZ61-3.0CNT

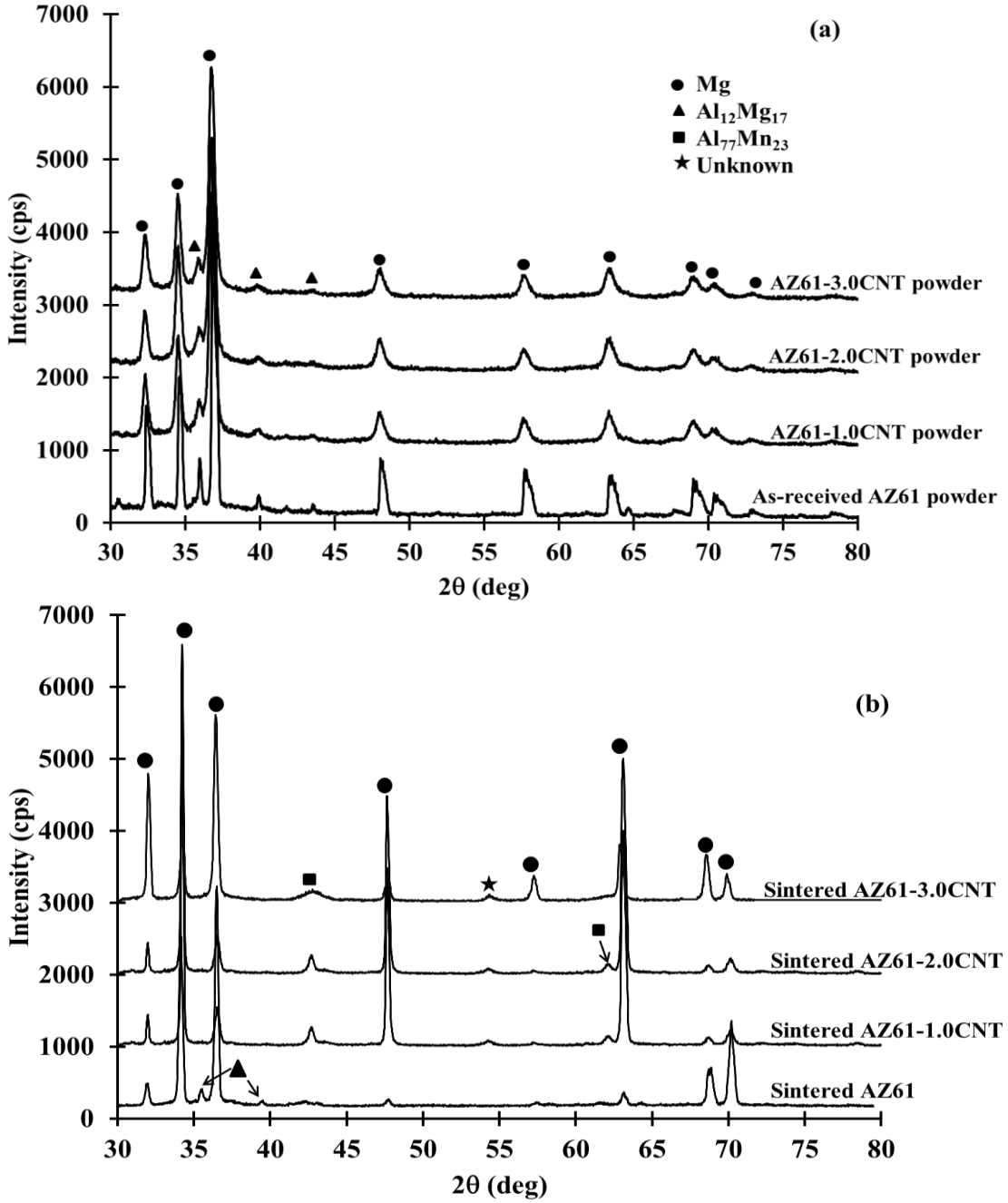

Fig.5 XRD diffractograms of (a) ball-milled monolithic and composite powders, and (b) sintered samples

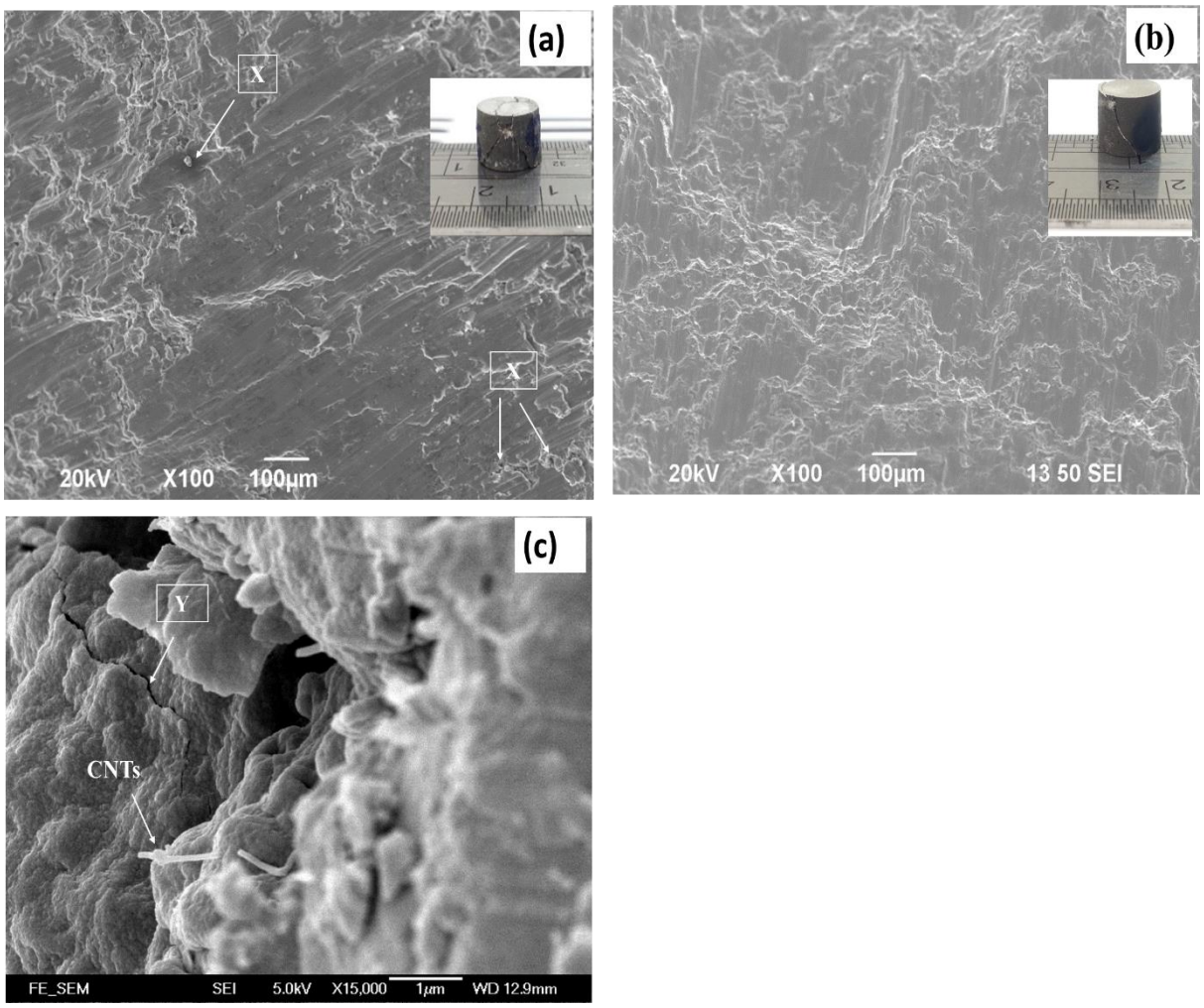

Fig.6 SEM fractographs showing (a) shear bands in monolithic AZ61 (**inset:** macroscopic failure cracks in a failed compressive sample); (b) mixed mode of shear and brittle failure in a composite sample (1 vol.% CNT) (**inset**: macroscopic failure crack in a failed compressive sample (1 vol.% CNT); and (c) FESEM image for fracture surface of a composite sample (1 vol.% CNT)

References

[1] Rashad M, Pan F, Tang A, Lu Y, Asif M, Hussain S, et al. Effect of graphene nanoplatelets (GNPs) addition on strength and ductility of magnesium-titanium alloys. J Magnes Alloy 2013;1:242–8.

[2] Hassan SF, Gupta M. Development of nano-Y2O3 containing magnesium nanocomposites using solidification processing. J Alloys Compd 2007;429:176–83.

[3] Luthringer BJC, Hort N, Feyerabend F. Metal matrix composites: magnesium. Wiley Encycl Compos 2012:1–23.

[4] Chen L, Tang CY, Ku HSL, Tsui CP, Chen X. Microwave sintering and characterization of polypropylene/multi-walled carbon nanotube/hydroxyapatite composites. Compos Part B Eng 2014;56:504–11.

[5] Kim MT, Rhee KY, Lee JH, Hui D, Lau AKT. Property enhancement of a carbon fiber/epoxy composite by using carbon nanotubes. Compos Part B Eng 2011;42:1257–61.

[6] Jyoti J, Basu S, Singh BP, Dhakate SR. Superior mechanical and electrical properties of multiwall carbon nanotube reinforced acrylonitrile butadiene styrene high performance composites. Compos Part B Eng 2015;83:58–65.

[7] Kim MT, Rhee KY, Park SJ, Hui D. Effects of silane-modified carbon nanotubes on flexural and fracture behaviors of carbon nanotube-modified epoxy/basalt composites. Compos Part B Eng 2012;43:2298–302.

[8] Dorri Moghadam A, Omrani E, Menezes PL, Rohatgi PK. Mechanical and tribological properties of self-lubricating metal matrix nanocomposites reinforced by carbon nanotubes (CNTs) and graphene – A review. Compos Part B Eng 2015;77:402–20.

[9] Habibi MK, Paramsothy M, Hamouda AMS, Gupta M. Using integrated hybrid (Al+CNT) reinforcement to simultaneously enhance strength and ductility of magnesium. Compos Sci Technol 2011;71:734–41.

[10] Zhang S, Chen Q, Fabrication of MWCNT incorporated Sn-Bi composite. Compos Part B Eng. 2014;58:275–278.

[11] Jenei P, Gubicza J, Yoon EY, Kim HS, Lábár JL. High temperature thermal stability of pure copper and copper-carbon nanotube composites consolidated by High Pressure Torsion. Compos Part A Appl Sci Manuf 2013;51:71–79.

[12] Bakshi SR, Lahiri D, Agarwal A. Carbon nanotube reinforced metal matrix composites - A review. Int Mater Rev 2010;55:41-64.

[13] Agarwal A, Bakshi SR, Lahiri D. Carbon Nanotubes: Reinforced Metal Matrix Composites. Boca Raton: CRC Press; 2010.

[14] Lau KT, Lu M, Hui D. Coiled carbon nanotubes: Synthesis and their potential applications in advanced composite structures. Compos Part B Eng 2006;37:437–48.

[15] Esawi A, Morsi K. Dispersion of carbon nanotubes (CNTs) in aluminum powder. Compos Part A Appl Sci Manuf 2007;38:646–50.

[16] Lloyd DJ. Particle reinforced aluminium and magnesium matrix composites. Int Mater Rev 1994;39:1–23.

[17] Oghbaei M, Mirzaee O. Microwave versus conventional sintering: A review of fundamentals, advantages and applications. J Alloy and Compd. 2010;494:175-189.

[18] Clark D, Sutton WH. Microwave processing of materials. Annu Rev Mater Sci. 1996;26:299-331.

[19] Eugene WW, Gupta M. Characteristics of aluminum and magnesium based nanocomposites processed using hybrid microwave sintering. J Microw Power Electromagn Energy. 2010;44:14-27.

[20] Roy R, Agrawal D, Cheng J, Gedevanishvili S. Full sintering of powdered-metal bodies in a microwave field. Nature. 399;1999:668-670.

[21] Gupta, M. And W.L.E. Wong. Microwaves and metals, John Wiley & Sons (Asia) Ptr Ltd, Singapore. 2007

[22] Agrawal D, Microwave sintering, brazing and melting of metallic materials. Sohn International Symposium; Advanced Processing of Metals and Materials Volume 4: New, Improved and Existing Technologies: Non-Ferrous Materials Extraction and Processing. 2006, pp 183-92.

[23] Nai MH, Goh CS, Nai SML, Wei, J., Gupta, M. Enhancement of mechanical properties by reinforcing magnesium with Ni-coated carbon nanotubes. ASME International Mechanical Engineering Congress and Exposition, Proceedings (IMECE), 2010;12:111-115.

[24] Thakur SK, Kwee GT, Gupta M. Development and characterization of magnesium composites containing nano-sized silicon carbide and carbon nanotubes as hybrid reinforcements. J Mater Sci 2007;42:10040–6.

[25] Habibi MK, Paramsothy M, Hamouda AMS, Gupta M. Enhanced compressive response of hybrid Mg–CNT nano-composites. J Mater Sci 2011;46:4588–97.

[26] Thakur SK, Srivatsan TS, Gupta M. Synthesis and mechanical behavior of carbon nanotube–magnesium composites hybridized with nanoparticles of alumina. Mater Sci Eng A 2007;466:32–7.

[27] Mayamaa T, Nodab M, Chibac R, Kurodad M. Crystal plasticity analysis of texture development in magnesium alloy during extrusion, Int J Plasticity. 2011;27:1916-1935.

[28] Menéndez JA, Arenillas A, Fidalgo B, Fernández Y, Zubizarreta L, Calvo EG, Bermúdez JM. Microwave heating processes involving carbon materials. Fuel Process Technol 2010;91:1–8.

[29] Higginbotham AL, Moloney PG, Waid MC, Duque JG, Kittrell C, Schmidt HK, Stephenson JJ, Arepalli S, Yowell LL, Tour JM. Carbon nanotube composite curing through absorption of microwave radiation. Compos Sci Technol 2008;68:3087–92.

[30] Suryanarayana C. Mechanical alloying and milling. Prog Mater Sci 2001;46:1–184.

[31] Frysz CA, Chung DDL. Improving the electrochemical behavior of carbon black and carbon filaments by oxidation. Carbon N Y 1997;35:1111–27. doi:10.1016/S0008-6223(97)00083-3.

[32] Wolff M, Ebel T, Dahms M. Sintering of magnesium. Adv Eng Mater 2010;12:829–36.

[33] Padmavathi C, Upadhyaya A, Agrawal D. Effect of microwave and conventional heating on sintering behavior and properties of Al-Mg-Si-Cu alloy. Mater Chem Phys 2011;130:449–57.

[34] ASTM Standard E384-11. Standard Test Method for Knoop and Vickers Hardness of Materials 2011.

[35] ASTM Standard E9-09. Standard Test Methods of Compression Testing of Metallic Materials at Room Temperature 2009.

[36] Oghbaei M, Mirzaee O. Microwave versus conventional sintering: a review of fundamentals, advantages and applications. J Alloys Compd 2010;494:175–89.

[37] Schneider F, Stolle A, Ondruschka B, Hopf H. The Suzuki−Miyaura reaction under mechanochemical conditions. Org Process Res Dev 2009;13:44–8.

[38] Choi HJ, Shin JH, Bae DH. The effect of milling conditions on microstructures and mechanical properties of Al/MWCNT composites. Compos Part A Appl Sci Manuf 2012;43:1061–72.

[39] Goh CS, Wei J, Lee LC, Gupta M. Ductility improvement and fatigue studies in Mg-CNT nanocomposites. Compos Sci Technol 2008;68:1432–9.

[40] Hung YP, Huang JC, Wu KJ, Tsao CYA. Strengthening and toughness of AZ61 Mg with nano SiO2 particles. Mater Trans 2006;47:1985–93.

[41] Ferguson JB, Sheykh-Jaberi F, Kim CS, Rohatgi PK, Cho K. On the strength and strain to failure in particle-reinforced magnesium metal-matrix nanocomposites (Mg MMNCs). Mater Sci Eng A 2012;558:193–204.

[42] Hassan SF, Gupta M. Development of high strength magnesium copper based hybrid composites with enhanced tensile properties. Mater Sci Technol 2003;19:253–9.

[43] Kondoh K, Fukuda H, Umeda J, Fugetsu B. Interfacial analysis of CNT reinforced AZ61

Mg alloy composites. In: Li X, Luo A, editors. Suppl. Proc. Vol. 1 Mater. Process. Interfaces TMS (The Miner. Met. Mater. Soc., vol. 1, NJ, USA: John Wiley & Sons, Inc.; 2012, p. 717–23.

[44] Viala JC, Claveyrolas G, Bosselet F, Bouix J. Chemical behaviour of carbon fibres in magnesium base Mg-Al alloys. J Mater Sci 2000;35:1813–25.

[45] Száraz Z, Trojanová Z, Cabbibo M, Evangelista E. Strengthening in a WE54 magnesium alloy containing SiC particles. Mater Sci Eng A 2007;462:225–9.

[46] Karbalaei Akbari M, Baharvandi HR, Mirzaee O. Nano-sized aluminum oxide reinforced commercial casting A356 alloy matrix: Evaluation of hardness, wear resistance and compressive strength focusing on particle distribution in aluminum matrix. Compos Part B Eng 2013;52:262–8.

[47] Rashad M, Pan F, Tang A, Asif M, Aamir M. Synergetic effect of graphene nanoplatelets (GNPs) and multi-walled carbon nanotube (MW-CNTs) on mechanical properties of pure magnesium. J Alloys Compd 2014;603:111–8.

[48] Hu J, Wu G, Zhang Q, Gou H. Mechanical properties and damping capacity of SiCp/TiNif/Al composite with different volume fraction of SiC particle. Compos Part B Eng 2014;66:400–6.

[49] Lloyd DJ. Aspects of fracture in particulate reinforced metal matrix composites. Acta Metall Mater 1991;39:59–71.

Figure Captions

Fig. 1: Cross-sectional view of the silicon carbide/graphite lined crucible and the position of a compact during microwave sintering.

Fig. 2: SEM micrographs of AZ61 alloy (a) as-received mainly spherical powder particles, (b) after 15 hours of milling showing flattened flake-like particles; and high magnification SEM images of (c) surface of AZ61-2.0CNT after 15 hours of milling, and (d) surface of AZ61-3.0CNT after 15 hours of milling.

Fig. 3: Raman spectra of (a) as-received CNTs; and AZ61-2.0CNTs milled for (b) 5 hours; (c) 10 hours; and (d) 15 hours

Fig. 4: Optical microstructures of the grain structure for a (a) monolithic AZ61; (b) AZ61-1.0CNT; (c) AZ61-2.0CNT; and (d) AZ61-3.0CNT

Fig. 5: XRD diffractograms of (a) ball-milled monolithic and composite powders, and (b) sintered samples

Fig. 6: SEM fractographs showing (a) shear bands in monolithic AZ61 (**inset:** macroscopic failure cracks in a failed compressive sample); (b) mixed mode of shear and brittle failure in a composite sample (1 vol.% CNT) (**inset**: macroscopic failure crack in a failed compressive sample (1 vol.% CNT); and (c) FESEM image for fracture surface of a composite sample (1 vol.% CNT)

Tables